Journal of Solid State Chemistry **149,** 434–442 (2000)
doi:10.1006/jssc.1999.8577, available online at http://www.idealibrary.com on IDEAL®

Mössbauer Effect Study of Copper Containing Nickel-Aluminate Ferrite

S. S. Ata-Allah,*,[1] M. K. Fayek,* H. S. Refai,* and M. F. Mostafa†

*Reactor and Neutron Physics Department, Nuclear Research Center, Atomic Energy Authority, Cairo, Egypt; and
†Physics Department, Faculty of Science, Cairo University, Giza, Egypt

Received July 16, 1999; accepted November 5, 1999

A series of spinel ferrite system $Ni_{1-x}Cu_xFeAlO_4$ with $(0.0 \leq x \leq 1.0)$ were prepared, checked by X-ray, and studied with ^{57}Fe Mössbauer effect spectroscopy in the 77–470 K temperature range. Characteristic spectra of paramagnetic, magnetic, and electronic types for the different compositions have been observed. Cation distribution obtained from spectral analysis revealed an inverse spinel system. Hyperfine parameters at 77 K were found to be temperature and concentration independent. At 293 K the hyperfine field decreases with increasing Cu concentration. Nèel point T_N obtained were found to decrease linearly with the compositional parameter x. Debye temperature θ_D of this ferrite system increases with increasing Cu content. The temperature dependence of the sublattice magnetization $\sigma_s(T)$ obeys a 1/3 power law in the $0.5 < T/T_N < 0.99$ temperature range. © 2000 Academic Press

INTRODUCTION

Diamagnetic substitutions in simple and mixed ferrites have received a great deal of attention over the past years (1, 2). The presence of nonmagnetic ions in spinel ferrites is found to alter their magnetic and electric properties. Such isomorphous substitutions in iron oxides are particularly apparent in their Mössbauer spectra, since these will drastically reduce magnetic interactions, resulting in lower magnetic ordering temperature and decreased magnetic field supertransfer (i.e., lower hyperfine fields) (3). Studies on aluminum magnetite $Al_xFe_{3-x}O_4$ showed that Al^{3+} ions have a *B*-site preference (4, 5). Also, studies of mixed nickel ferrites Ni–Cu show interesting results of cation distributions and magnetic properties (6).

The present work reports the results of Mössbauer-effect studies of Cu^{2+}–substituted nickel-aluminate ferrites $Ni_{1-x}Cu_xAl_yFe_{2-y}O_4$ (with $0.0 \leq x \leq 1.0$) and $y = 1.0$). Our goal is to shed more light on the microscopic picture of the magnetic ordering in these diluted ferrimagnets. The present activity is part of a program to study the effect of introducing nonmagnetic cations in Ni–Cu ferrites.

EXPERIMENTAL DETAILS

Six polycrystalline samples of the studied compounds were prepared by solid–state reactions using Fe_2O_3, NiO, CuO, and Al_2O_3 (with purity $\geq 99.99\%$) as starting materials. The mixture of the oxide powders is prefired at (950–1100°C), depending on the CuO content, for 72 h. The product is reground and fired again under the same conditions to improve homogeneity. The final powders are pressed into pellets and sintered at (1000–1200°C) for 8 h, then slowly cooled to room temperature. X-ray powder diffraction measurements are obtained using Co$K\alpha$ radiation, and their analysis showed that the products are crystallized in a single-phase cubic spinel. The ME spectra of the samples are recorded with a time mode spectrometer, using a constant acceleration drive and a personal computer analyzer (PCA II-card with 1024 channel). The source is ^{57}Co in Rh matrix with an initial activity 50 mCi. Metallic iron and α-Fe_2O_3 spectra are used for the calibration of both observed velocities and hyperfine magnetic fields. The absorber thickness is approximately 10 mg/cm^2 of natural iron. Measurements as a function of temperature are made using Oxford liquid-nitrogen cryostat Model (DN1726) with a Model ITC^{502} temperature controller and a variable temperature oven with a VF100 temperature controller. In the low- and high-temperature measurements, the temperature was maintained constant to ± 0.1 K, and the vacuum was better than 2×10^{-5} mm of Hg using a turbo molecular pump Model (BH2-60). Spectra were analyzed using the Mos-90 computer program (7). The areas of both tetrahedral and octahedral subspectra of the Fe^{3+} were used for determination of cation distribution for each composition.

[1] To whom correspondence should be addressed. E-mail: ssataallah@hotmail.com.

0022-4596/00 $35.00

RESULTS AND DISCUSSIONS

Figure 1 shows the X-ray powder diffraction patterns of the prepared samples. The diffraction peaks are fitted by modified Gaussian functions, and the lattice parameters are obtained by fitting at least 10 diffraction peaks using standard least-squares methods. The result of indexing the X-ray powder diffraction patterns showed that the nominal composition structure with different concentration are single-phase cubic with no additional lines corresponding to any other phases. The variation of the lattice parameter a with the compositional parameter x is given in Table 1, where a is found to increase with increasing Cu concentration. This is due to the fact that the Pauling ionic radius of Cu^{2+} (0.72 Å) is greater than that of Ni^{2+} (0.69 Å).

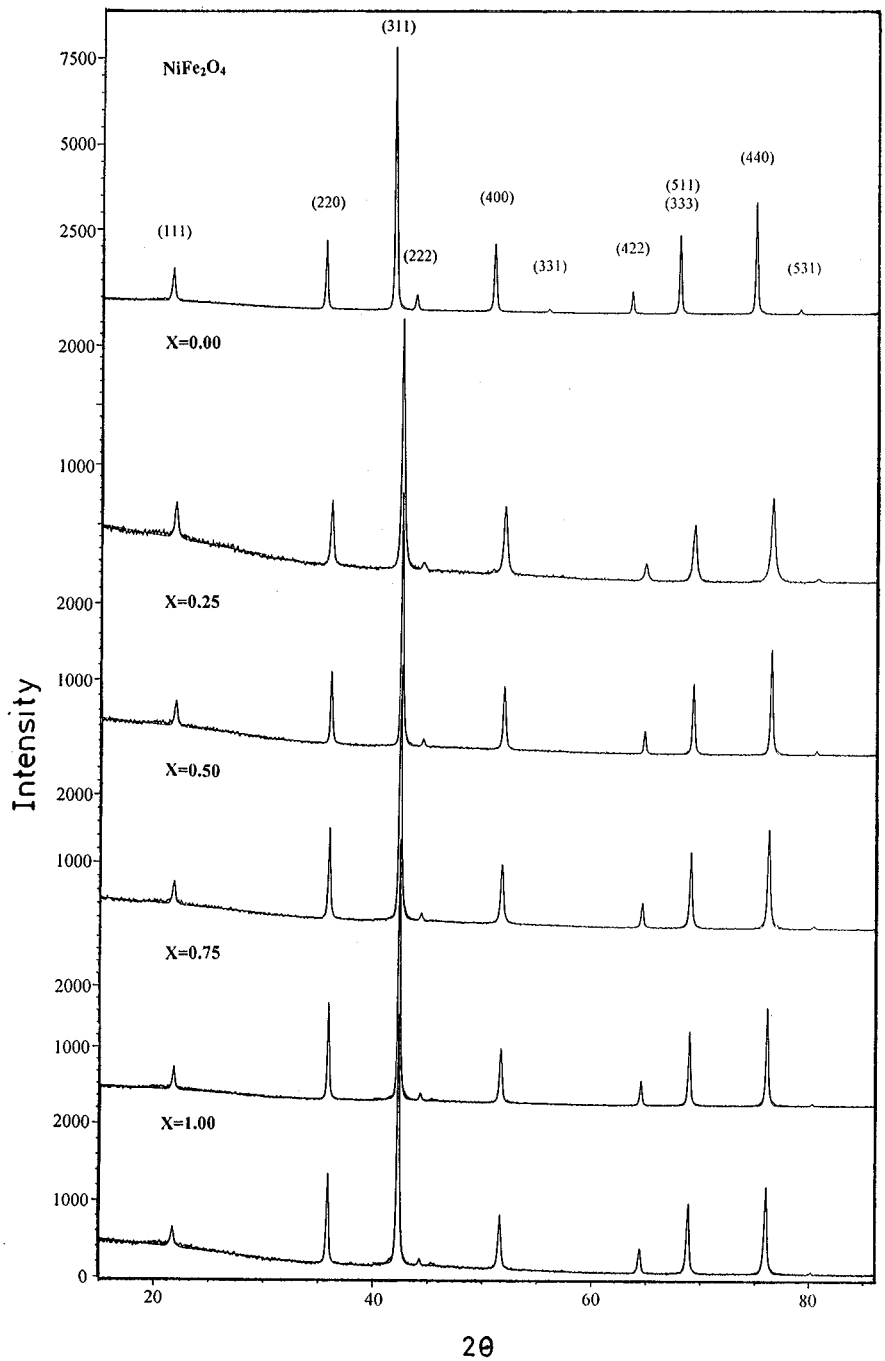

FIG. 1. X-ray powder diffraction patterns at room temperature for $NiFe_2O_4$ and $Ni_{1-x}Cu_xFeAlO_4$ spinel ferrites.

TABLE 1
Lattice Parameters a of $Ni_{1-x}Cu_xFeAlO_4$ Spinel Ferrites

x	Lattice constant a (Å)
0.00	8.1891 ± 0.004
0.25	8.1957 ± 0.0038
0.50	8.2082 ± 0.0044
0.75	8.2186 ± 0.0041
1.00	8.2264 ± 0.005

The analysis of ME spectra for the $Ni_{1-x}Cu_xFeAlO_4$ is based on the general results previously reported on spinel ferrites. To identify and distinguish the different spectral lines from iron on tetrahedral A- and octahedral B-sites and determine their ME parameters in order to discuss their nuclear and magnetic behavior, the following points are first considered:

1. The magnetic hyperfine splittings contain three pairs of doublets and each is separated according to the ratio; $\delta_1 : \delta_2 : \delta_3 : = 1 : 0.58 : 0.16$; where, δ_1 is the relative separation between peaks 1 and 6, δ_2 between peaks 2 and 5, and δ_3 is that between peaks 3 and 4.

2. The hyperfine fields H_{hf} for both A and B sites are determined from the separation between the centroids of the peaks in each Zeeman pattern.

3. For magnetically ordered spinel ferrites, the magnetic hyperfine field due to Fe at A sites H_{hfA} is usually smaller than that of Fe at B sites H_{hfB} (8).

4. The Zeeman pattern with the smaller isomer shift exhibits the smaller hyperfine field (in agreement with the generally accepted correlation between isomer shifts and hyperfine fields in ferrites) (9).

5. In most spinels, there is a small deviation from cubic symmetry maintained about tetrahedral A sites. This leads to a quadrupole splitting (QS) of the nuclear level of B-site iron and hence to a doublet ME spectrum (10), while Fe at A sites produce a single line.

6. The recoilless free fractions of A- and B-site iron are roughly equal at a particular temperature (11).

7. The line width (full width at half-maximum FWHM) of the tetrahedral component in spinel ferrites is less than that of the octahedral component (12).

ME spectrum at room temperature for the stoichiometric $NiFe_2O_4$ sample consists of two clearly split Zeeman sextets due to Fe^{3+} at A and B sites as shown in Fig. 2. ME spectra at 77 K for $Ni_{1-x}Cu_xFeAlO_4$ spinel ferrites with composition range $0.0 \leq x \leq 1.0$ exhibit well-defined absorption lines. These spectra are fitted with one sextet due to Fe^{3+} at one of the two distinct crystallographic sites and are attributed to the tetrahedral A sites on the basis of the isomer shift (IS) and the hyperfine field H_{hf} values. ME spectra at room temperature for these samples showed a relaxed

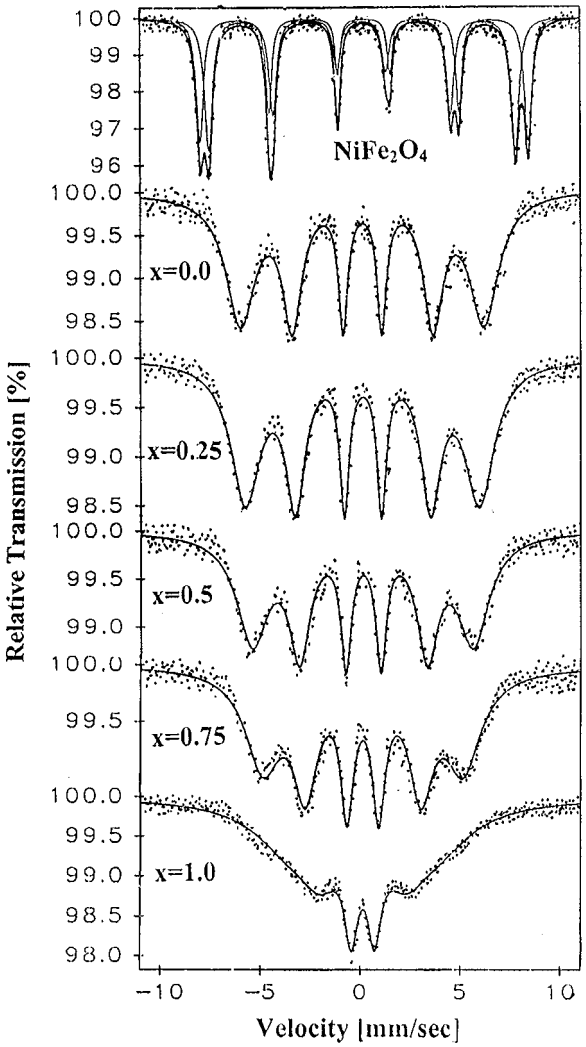

FIG. 2. ME spectra of ^{57}Fe for $NiFe_2O_4$ and $Ni_{1-x}Cu_xFeAlO_4$ ferrite system at 293 K.

spectra, where the relaxation effect is found to increase as the copper concentration (x) increases as shown in Fig. 2. The dominant spin lattice relaxation in the relaxed spectra may be due to the presence of the octahedral quadrupole interaction (13). Representative ME spectra for compounds with ($x = 0.25$ and 0.5) in the temperature range 77 K up to their magnetic transition temperatures are shown in Figs. 3 and 4.

Cation Distribution

The fraction of iron ions at a distinct crystallographic site can be determined from the ME spectra by knowing the area under the resonance lines due to these ions. In order to get the correct intensity ratio, the A- and B-site patterns should be well separated. In the simple ferrite $NiFe_2O_4$ sample where a well-resolved ME spectrum into

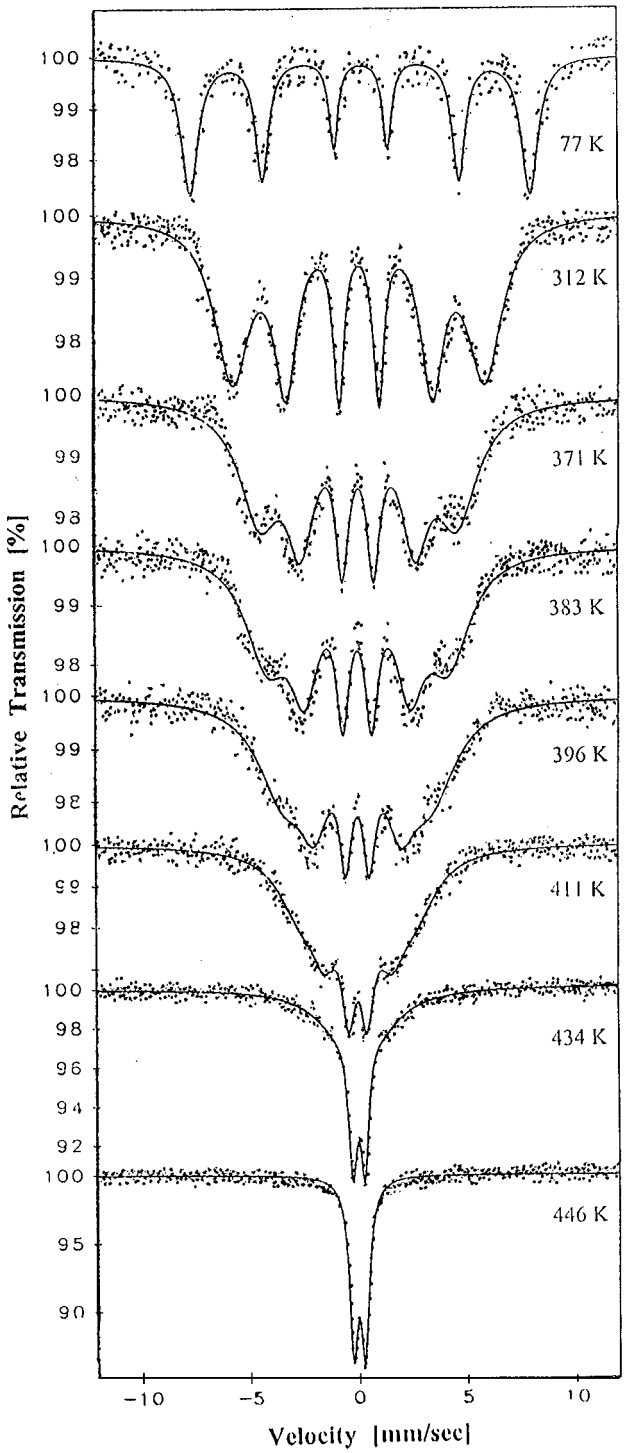

FIG. 3. ME spectra of ^{57}Fe for $Ni_{0.75}Cu_{0.25}FeAlO_4$ samples at different temperatures.

two Zeeman sextets with equal areas of *A* and *B* subspectra, as shown in Fig. 2, gives a cation distribution as $Fe^{3+}[Ni^{2+}Fe^{3+}]O_4^{2-}$ for this simple ferrite. Since, Ni^{2+} and Al^{3+} ions on the basis of the site-preference energy data (14), are present at *B* sites. Thus, cation distribution of the present spinel ferrite system $Ni_{1-x}Cu_xFeAlO_4$ is $(Fe^{3+})[Ni^{2+}_{1-x}Cu^{2+}_xAl^{3+}]O_4^{2-}$. This was deduced from ME spectra at 77 K, where a resolved spectra fitted to one sextet due to Fe^{3+} ions at the *A* site. This means that the introduction of Al in $NiFe_2O_4$ replaces Fe at the octahedral *B* sites. Also, the substitution of Cu^{2+} in these spinel ferrites results in replacing Ni at the *B* site. These results of the deduced cation distribution give evidence of a complete inverse spinel in this system.

Quadrupole Interaction

The presence of chemical disorder in the spinel structure will produce an electric field gradient (EFG) of varying

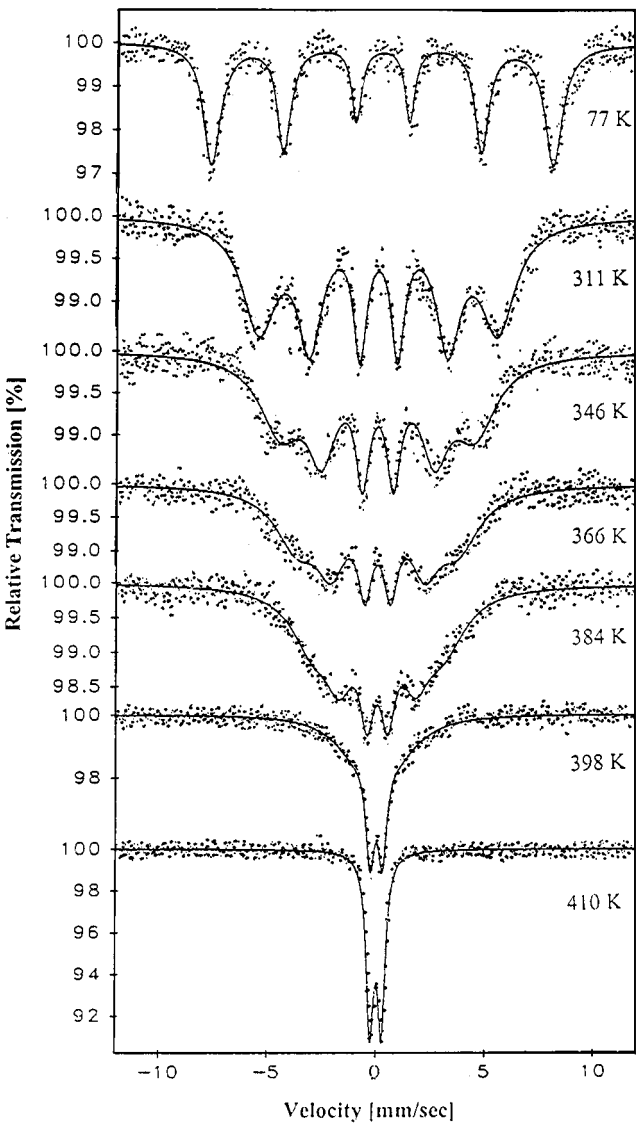

FIG. 4. ME spectra of ^{57}Fe for $Ni_{0.5}Cu_{0.5}FeAlO_4$ ferrites at different temperatures.

TABLE 2
Hyperfine Parameters of $Ni_{1-x}Cu_xFeAlO_4$ at 77 and 293 K

	Q.S. [mm/s]		I.S. [mm/s]		H_{hf}(kOe)	
x	77 K	293 K	77 K	293 K	77 K	293 K
0.00	-0.031 ± 0.0021	-0.012 ± 0.0027	0.408 ± 0.011	0.31 ± 0.014	446.9 ± 0.09	394.6 ± 0.14
0.25	-0.028 ± 0.0018	-0.027 ± 0.0011	0.391 ± 0.009	0.31 ± 0.006	443.7 ± 0.08	379.8 ± 0.06
0.50	-0.001 ± 0.0016	-0.018 ± 0.0016	0.402 ± 0.008	0.32 ± 0.01	447.1 ± 0.07	359.7 ± 0.09
0.75	-0.021 ± 0.003	-0.003 ± 0.0028	0.401 ± 0.015	0.34 ± 0.015	436.4 ± 0.14	327.2 ± 0.18
1.00	-0.007 ± 0.002	-0.022 ± 0.007	0.431 ± 0.01	0.36 ± 0.04	436.3 ± 0.1	243.8 ± 0.41

magnitude, direction, sign, and symmetry and a resulting distribution in the QS. In other words the EFG at ^{57}Fe nucleus arises from the asymmetrical charge distribution surrounding the ion. However, since an Fe^{3+} ion has a half-filled $3d$ shell ($3d^5$), the EFG in this case can arise only from an asymmetric charge distribution surrounding the iron ion. In a cubic system having Fe^{3+} at both A and B sites, the A site shows a quadrupole splitting due to the asymmetric charge distribution from the 12 B neighbors. The Fe^{3+} ion at the B site has trigonal symmetry, and therefore the B sublattice exhibits an electric field gradient with its principal component V_{zz} along the [111] direction. This EFG may arise from depature of the six nearest anion neighbors from their ideal octahedral symmetry and the nonspherical distribution of charges on the next-nearest cation and anion neighbors of the B site. In the present work, there is no QS at low temperature [77 and 293 K] for the ferrite system $Ni_{1-x}Cu_xFeAlO_4$ as given in Table 2. This could be explained due to the overall cubic symmetry of the spinel ferrite and randomness of chemical disorder, there will be equal probability for small QS's of opposite signs. Hence, the centers of the Zeeman lines will not change, and consequently there will be no net observable QS. Figure 5 shows the variation of QS with temperature, where the QS is present as shown just below and above the magnetic transition T_N. The paramegnetic spectra (taken above the transition temperature T_N) for $Ni_{1-x}Cu_xFeAlO_4$ spinels are analyzed in terms of a quadrupole doublet corresponding to an Fe^{3+} ion at the A site. The determined value of the quadrupole splitting for the tetrahedral ions in the different samples (QS $= 1/2\ \Delta E_Q$, where ΔE_Q is the actual separation of the quadrupole doublet) is given in Table 3. It is noticed that QS, and thus the magnitude of the EFG at the tetrahedral site decreased with increasing Cu content x until $x = 0.5$, then it increased. This could be attributed to the fact that the oxygen parameter U changes with the introduction of the Cu^{2+} ion with larger ionic radius (0.72 Å) to replace the smaller Ni^{2+} ions (0.69 Å) in the octahedral site. The change of temperature from (77 up to ~ 470 K) causes no detectable variation on the value of the QS (within experimental error). This means that only the contribution of the unsymmetrical charge distribution of the neighboring ions (oxygen) in the crystal has an effect on QS. Moreover, it shows also the absence of any significant lattice distortion during this range of temperature.

Isomer Shift

The obtained IS values for $Ni_{1-x}Cu_xFeAlO_4$ spinel ferrites at room temperature given in Table 2 are in the 0.31–0.36 mms^{-1} range. These values are typical for that of Fe^{3+} ions at tetrahedral A sites of spinel structure (15–17). There is no significant change of IS values with copper content observed in this spinel system. This means that the s electron charge distribution of Fe ions is negligibly influenced by copper substitution. The Mössbauer isomer shift consists of two parts: the temperature-independent part, the isomer shift δ_{IS}, and the temperature-dependent part, the second-order Doppler shift, δ_{SOD}. The latter results from the relativistic motion of the emitting nuclei. The temperature variation of the isomer shift is shown in Fig. 6. The results are best fitted to one line. The linear regression for this line is listed in Table 4 together with some Mössbauer parameters. The temperature shift is proportional to the ^{57}Fe nuclear vibrational energy. The temperature coefficients $(1/v)\ (\partial v/\partial T)$ calculated from the slope of the temperature shift for all compounds under investigation are also given in Table 4. Thus, the slope of the curve of Fig. 6 are proportional to the ^{57}Fe nuclear specific heat C_p. Using the relation for harmonic forces (18)

$$C_p = -(1/v)(\partial v/\partial T)\, 2Mc^2 \ [\text{erg/(mole deg)}]$$

one gets the specific heat of iron nuclei. Here, M is the nuclear weight of ^{57}Fe, c is the velocity of light in cm/s, and v is the frequency of the γ ray. The calculated values of C_p are given in Table 4. They increase with increasing Cu content and compare reasonably well with the expected value of 6 cal/mole degrees for ^{57}Fe at the mid range of the substitution ($x = 0.5$). The recoilless fraction, f(measured as

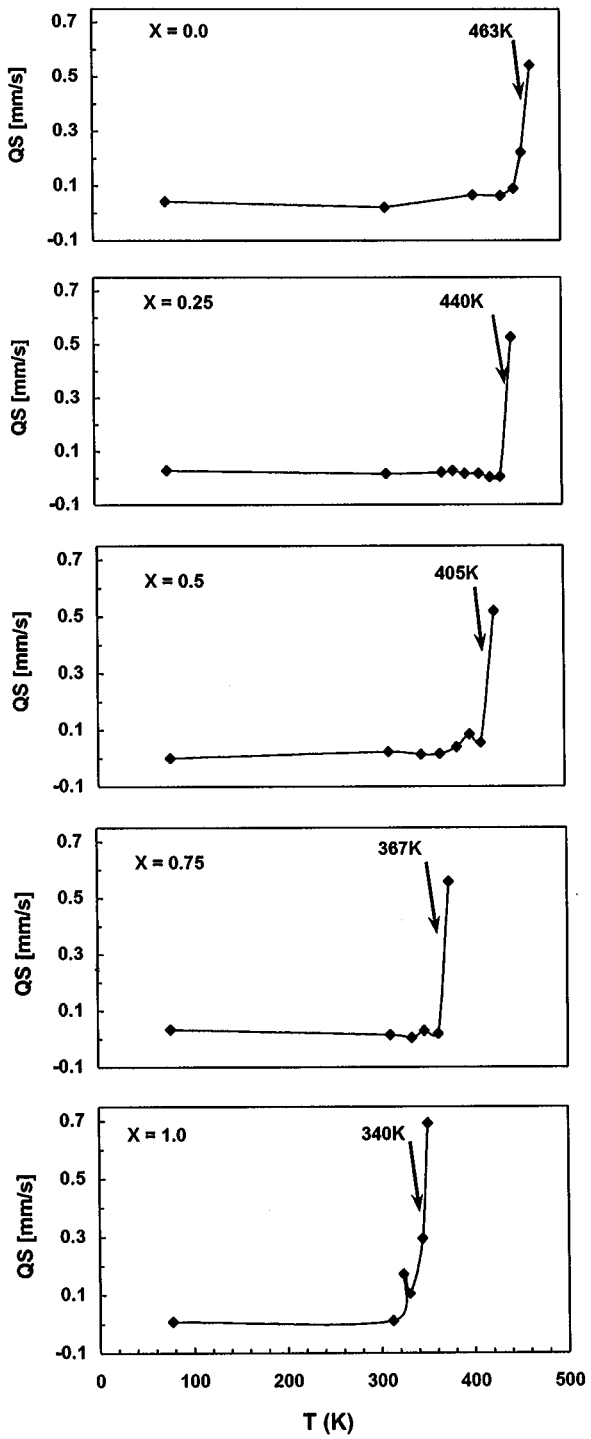

FIG. 5. Variation of QS with temperature for $Ni_{1-x}Cu_xFeAlO_4$ compounds.

the area (A) under the resonance curve for a fixed counting time), can be related to the Debye lattice temperature, θ_D, (19) by the relationship

$$f(\alpha, A) = \exp[-6E_\gamma T/(k\theta_D^2)] = \exp[-3E_\gamma T/(M_{\text{eff}} c^2 k\theta_D^2)].$$

This leads to the following expression for the Debye temperature:

$$\theta_D = [3E_\gamma^2/(M_{\text{eff}} c^2 k)]^{1/2} (-\partial \ln A/\partial T)^{1/2}.$$

A plot of $\ln A$ versus T is shown in Fig. 7. A least-squares fit results in one straight line in the same temperature region as found for the isomer shift data. The linear regression is listed in Table 4, from which one notices that the Debye temperature increases with increasing Cu concentration in this ferrite system.

Hyperfine Fields

The hyperfine magnetic field at the iron nucleus is assumed to be proportional to the spontaneous magnetization of the sublattice to which the particular nucleus belongs. The hyperfine field H_{hf} measured by the Mössbauer effect consists of three contributions: $H_{hf} = H_{core} + H_{dip} + H_{shift}$, where H_{core} results from the polarization of s electrons by the magnetic moments of the d electrons. This field is larger for free ions than for ions in a crystal because of covalency. H_{dip} represents the dipolar fields produced by the surrounding magnetic ions. This field depends on the distribution of the cation over A and B sites. H_{shift} is the supertransferred hyperfine fields at a central cation, and it originates from the magnetic moments of the nearest-neighbor cations, i.e., from the intersublattice contributions h_{AA} and h_{BB} and the intersublattice contributions h_{AB} and h_{BA}. The hyperfine field H_{hf} values at 293 and 77 K for $Ni_{1-x}Cu_xFeAlO_4$ spinel ferrites are given in Table 2. Note that the hyperfine field H_{hf} decreases as the Cu content x increases at 293 K, whereas at 77 K there is no significant change in H_{hf}, which remains almost constant at a value ≈ 442 kOe. This means that at 293 K the intersublattice contributions h_{AB} and h_{BA} are predominant and the introduction of Cu^{2+} in place of Ni^{2+} at the octahedral sites results in a decrease of these intersublattice contributions. But at 77 K, the intersublattice contributions h_{AA} is the most predominant. So, there is no significant change in H_{hf} with Cu content at 77 K. The Nèel temperatures T_N obtained are listed in Table 4. It shows that as the copper concentration x increased, T_N decreased linearly. This is in agreement with Gilleo studies for superexchange interaction for various oxide (17), which indicated

TABLE 3
Quadrupole Splitting at the A Site of the Paramagnetic ME Spectra of $Ni_{1-x}Cu_xFeAlO_4$ Ferrites

X	0.0	0.25	0.50	0.75	1.00
QS [mm/s]	0.5436 ± 0.0065	0.5270 ± 0.0036	0.5196 ± 0.0035	0.5335 ± 0.0041	0.6930 ± 0.006

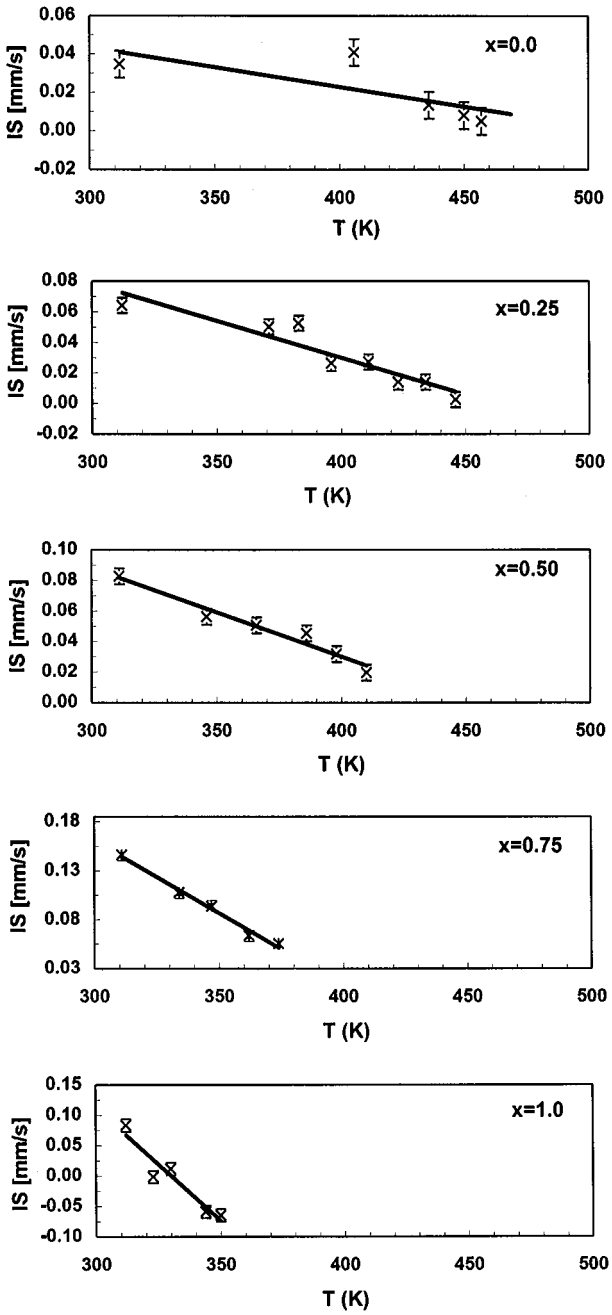

FIG. 6. Least-squares fit of the variation of isomer shift with temperature for $Ni_{1-x}Cu_xFeAlO_4$.

that Nèel point depends primarily upon the number of Fe^{3+}–O^{2-}–Fe^{3+} linkages. In $Ni_{1-x}Cu_xAl_yFe_{2-y}O_4$ ferrite spinels, T_N depends also upon the number of Ni^{2+}–O^{2-}–Ni^{2+} linkages. The introduction of Cu in these samples in place of Ni decreases the number of Ni^{2+}–O^{2-}–Ni^{2+} linkages and therefore Nèel temperature. The values of the determined hyperfine magnetic fields $[H(T)/H(0)]$ versus T/T_N are plotted in Fig. 8. A good agreement is obtained for the reduced hyperfine magnetic field versus T/T_N plot for these compounds with the Brillouin function $B_s = 5/2$, reflecting the same spin state for iron situated at the A site, even in the high temperature range. It may be concluded that the electronic relaxation in the $|\pm 5/2\rangle$ electronic crystal field levels of $^6S_{5/2}$ $^{57}Fe^{3+}$ ions is large enough compared to the nuclear Larmer pre cession time. The relative sublattice magnetization as a function of temperature T has been found both in various

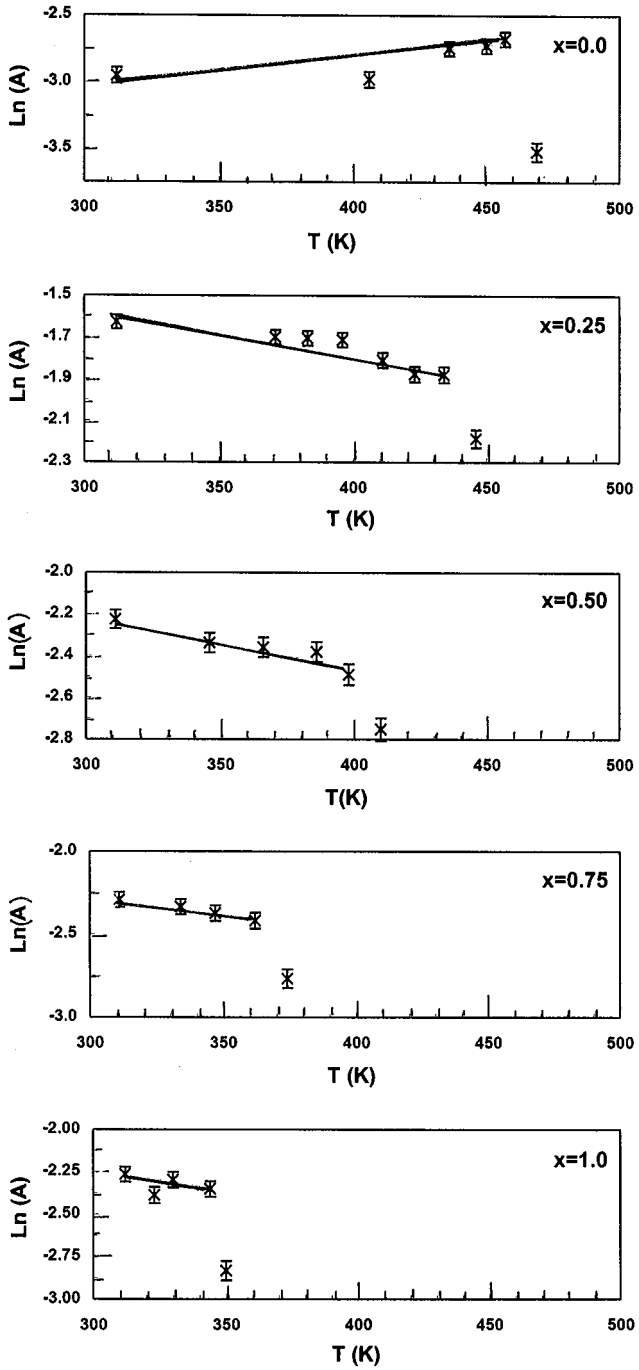

FIG. 7. Least-squares fit of the temperature variation of the recoilles fraction of $Ni_{1-x}Cu_xFeAlO_4$ spinels.

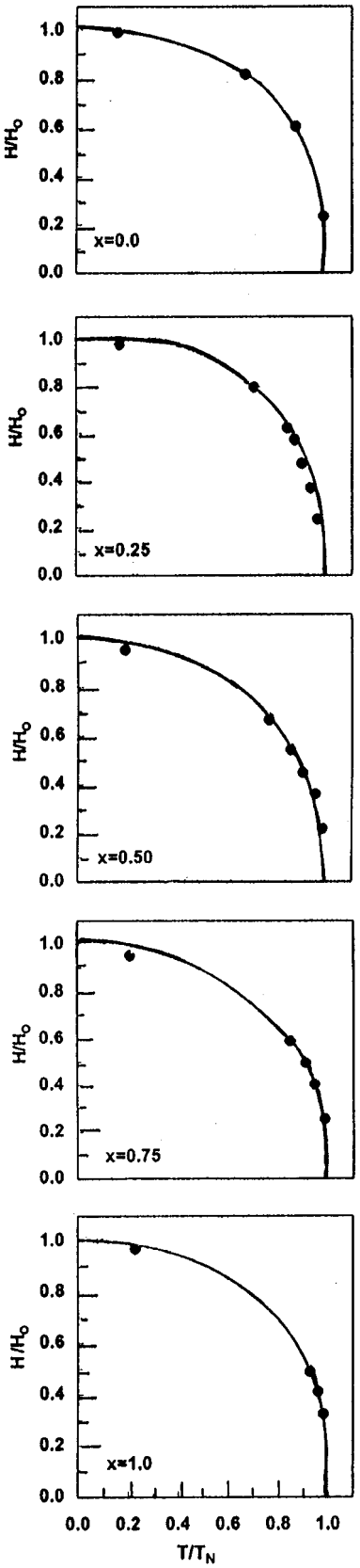

FIG. 8. Internal magnetic field H(T) normalized to H(0) as a function of the reduced temperature T/T_N for $Ni_{1-x}Cu_xFeAlO_4$ spinels.

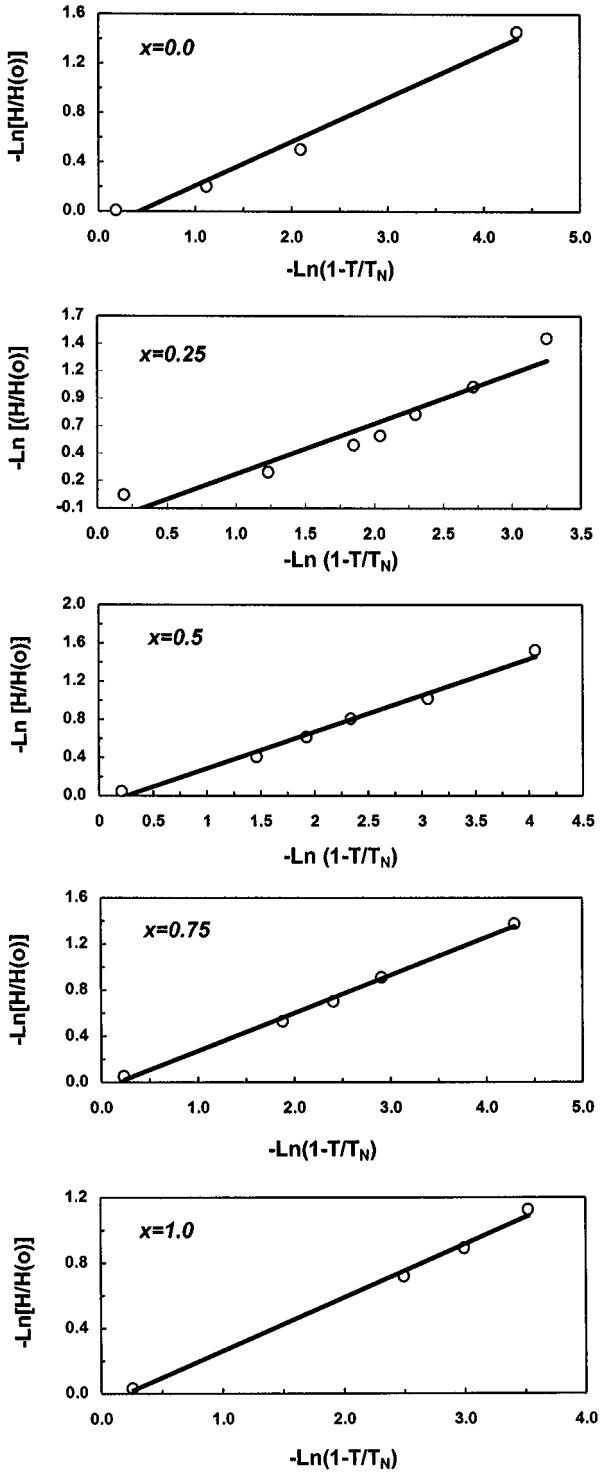

FIG. 9. The one-third power law applied to the A site for $Ni_{1-x}Cu_xFeAlO_4$.

theories (20, 21) and experimentally (22, 23) to follow the equation

$$\sigma_s(T)/\sigma_s(0) = D\,[1-(T/T_N)]^{\beta},$$

TABLE 4
Some Mössbauer Parameters of $Ni_{1-x}Cu_xFeAlO_4$ Compounds

X	T_N (K)	IS regression (mm/s)	$(1/v)(\partial v/\partial T)$ $\times 10^{15}$	C_p	LnA regression	θ_D (K)	β
0.00	463	2×10^{-4} T	-0.75	1.82	1.6×10^{-3} T	155	0.357
0.25	440	5×10^{-4} T	-1.86	4.55	2×10^{-3} T	215	0.459
0.50	404	6×10^{-4} T	-2.24	5.46	2.1×10^{-3} T	233	0.383
0.75	368	1.5×10^{-3} T	-5.59	13.6	2.5×10^{-3} T	335	0.328
1.00	343	3.7×10^{-3} T	-13.79	33.6	2×10^{-3} T	841	0.327

where $\sigma_s(T)$ is the sublattice magnetization at a given temperature. In Fig. 9, the internal field $H(T)/H(0)$ versus $[1-(T/T_N)]$ for $Ni_{1-x}Cu_xFeAlO_4$ spinel ferrites is plotted on a double logarithmic scale. These plots are straight lines in the range $0.5 < T/T_N < 0.99$. Here, the upper bound is determined by the resolution of spectra in the experiment. The exponent β obtained from the logarithmic plots is given in Table 4. The error in β is found to be ± 0.005, which comes from the experimental uncertainties in the measurements of the temperature and the internal field. On the average, $\beta = 0.358$, which is thus quite close to 1/3. The analysis of ME data showed that the one-third power law (23), which describes sublattice magnetization at $T/T_N > 0.5$, is valid for the studied compositions.

REFERENCES

1. A. Navrotsky and O. J. Kleppa, *J. Inorg. Nucl. Chem.* **29,** 2701 (1967).
2. S. K. Kulshrestha and G. Ritter, *J. Mater. Sci.* **20,** 821 (1985)
3. A. A. Choni, A. I. Etyhhand, and A. A. Mohamed, *Proc. Int. Conf. Ferrites* **5,** 216 (1980).
4. U. Schwertmann, *Adv. Soil Sci.* **1,** 171 (1985).
5. M. K. Fayek, S. S. Ata-Allah, and H. S. Refai, *J. Appl. Phys.* **85,** 325 (1999).
6. N. N. Greenwood and T. C. Ggibb, "Mössbauer Spectroscopy," pp. 259–268. Chapman and Hall, London, 1971.
7. B. J. Evans, "Mössbauer Effect Methodology 4," pp. 139–158. Plenum Press, New York, 1968.
8. C. D. Spenser and D. Shroeer, *Phys. Rev. B* **9,** 3658 (1974).
9. C. A. Sawatzky, F. Vanderwoude, and A. H. Morrish, *Phys. Rev.* **183,** 83 (1969).
10. M. K. Fayek, *Proc. ICAME* 253 (1982).
11. R. K. Puri, V. K. Babber, and R. G. Mendiratte, *Proc. Int. Conf. Ferrites* **5,** 329 (1989).
12. A. Miller, *J. Appl. Phys.* **30,** 245 (1959).
13. B. J. Evans and S. S. Hafner, *J. Phys. Chem. Solids* **29,** 1850 (1968).
14. D. C. Khan, R. C. Srivastava, and A. R. Das, *J. Phys. Condens. Matter* **4,** 1379 (1992).
15. P. R. Edward, C. E. Jonhson, and R. J P. Williams, *J. Chem. Phys.* **47,** 2074 (1967).
16. R. V. Pound and G. A. Rebka, *Phys. Rev. Lett.* **4,** 274 (1960).
17. M. A. Gilleo, *J. Phys. Chem. Solids* **13,** 33 (1960).
18. M. Eibschultz, S. Shtrikman, and D. Treves, *Phys. Rev.* **156,** 562 (1967).
19. M. F. Mostafa and R. M. Emrick, *Physica B* **210,** 67 (1995).
20. J. W. Essam and M. F. Fisher, *J. Chem. Phys.* **38,** 802 (1963).
21. E. Callen and H. B. Callen, *J. Appl. Phys.* **36,** 1140 (1965).
22. D. G. Howard, B. D. Dunlap, and J. G. Dash, *Phys. Rev. Lett.* **15,** 628 (1965).
23. M. Eibschultz, S. Shtrikman, and D. Treves, *Solid State Commun.* **4,** 147 (1966).